OTREC2019: Convection over the East Pacific and Southwest Caribbean

Enter authors here: Ž. Fuchs-Stone[1,2], D. J. Raymond[1,2], and S. Sentić[1]

[1]Climate and Water Consotrium, New Mexico Tech, 801 Leroy Place, Socorro, NM.

[2]Physics Department, New Mexico Tech, 801 Leroy Place, Socorro, NM.

Corresponding author: Željka Fuchs-Stone (zeljka.fuchs@nmt.edu)

Key Points:

- Thermodynamic parameters instability index and saturation fraction show ani-correlation.
- Moisture quasi-equilibrium theory explains the control of convection in the region.
- Vertical mass flux profiles are bottom heavy for developing convection and top heavy for decaying convection.

Abstract

Moisture quasi-equilibrium theory postulates that the instability index, a measure of low to mid-tropospheric moist convective instability, is inversely proportional to saturation fraction, a good proxy for precipitation. We looked at thermodynamic properties for 16 convective events from dropsonde data collected during the field project Organization of Tropical East Pacific Convection (OTREC). OTREC2019 performed 22 flights in the Eastern Pacific and Southwest Caribbean out of Costa Rica using the NSF/NCAR Gulfstream V aircraft. Convective available potential energy and saturation fraction show weak anti-correlation, while the instability index and saturation fraction are more strongly anti-correlated. This supports the moisture quasi-equilibrium hypothesis.

Vertical mass flux profiles are calculated for all 16 convective events (8 convective cases in the tropical Eastern Pacific, 5 off the Pacific coast of Colombia and 3 in the Southwest Caribbean). Every developing convective case has a bottom-heavy vertical mass flux profile and every decaying case has top-heavy profile.

Plain Language Summary

Understanding and modeling the physics of tropical atmospheric convection still poses a big challenge. Things are complicated over the tropical oceans because there is no easy way to gather data. Field projects such as the one presented in this paper, Organization of Tropical East Pacific Convection (OTREC2019) are of great importance to our scientific community for this reason. During OTREC, 22 research flights were performed over East Pacific and Southwest Caribbean gathering data from 13 km to surface. This paper presents early results that will help us understand the physics of convection and improve our weather and climate models.

1 Introduction

Understanding and describing the nature of convection in the East Pacific ITCZ remains a challenge. Riehl et al. (1951), Lindzen and Nigam (1987), Battisti et al. (1999), Tomas et al. (1999), Stevens et al. (2002), Back and Bretherton (2009) suggest that Ekman balance theory plus downward momentum transfer from above the boundary layer are responsible for the ITCZ. Alternatively, Emanuel (1986, 1987) and Neelin et al. (1987) propose that surface moist entropy fluxes drive convection. This mechanism is called WISHE (wind-induced surface heat exchange), (Yano and Emanuel, 1991). This paper presents early results from the OTREC2019 (Organization of Tropical East Pacific Convection) field program that cast light on this issue.

Previous to OTREC2019, the most recent field project to study East Pacific convection was EPIC2001 (East Pacific Investigation of Climate), which took place from September 1 to October 10, 2001. One of the goals was to determine variability, strength and location of deep convection and the structure of the boundary layer. The program had a large oceanic component as well. (For more details on EPIC see Raymond et al. (2004).) During EPIC, two aircraft, NCAR C-130 and NOAA P-3, were deployed from Huatulco, Mexico. The P-3 was used to map the ITCZ by flying a grid pattern at 1900 m. C-130 flew along 95 W to the equator at low altitude, but in its return leg dropped dropsondes from 6300 m height. It also flew missions targeted at individual convective clusters.

Raymond (2017) studied Eastern Pacific ITCZ based on EPIC2001 C-130 data and suggested that thermodynamic parameters such as saturation fraction and instability index are likely predictors of the local properties of the environment and that the interaction of ensembles of convection with the environment depends only on the local properties of the environment. However, EPIC C-130 data were limited to the lower troposphere at a single longitude, which introduced significant limitations.

The saturation fraction is a kind of column relative humidity and is defined as precipitable water over the saturated precipitable water

$$SF = \frac{\int r dp}{\int r_s dp}$$

where r is the mixing ratio, r_s is the saturation mixing ratio and p is the pressure. It is a measure of the amount of moisture in the atmospheric column and is a good proxy for precipitation, (Bretherton et al., 2004).

Instability index is defined as:

$$II = s_{low} - s_{high}$$

where s_{low} and s_{high} are respectively the saturated moist entropy averaged over the altitude ranges of 1-3 km and 5-7 km. It is a measure of low to mid-tropospheric moist convective instability. Lower, but still positive, values are associated with more rainfall, (Raymond et al., 2014). Based on T-PARC/TCS08 (THORPEX Asian Regional Campaign/Tropical Cyclone Structure experiment) and PREDICT (PREDepression Investigation of Cloud systems in the Tropics), Raymond et al. (2014) also find that decrease in instability index is associated with bottom-heavy vertical mass flux profiles.

The tropical East Pacific ITCZ is unique due to the existence of a strong meridional sea surface temperature (SST) gradient with lowest SSTs occurring on the equator (Figure 1). Both the form and the forcing of deep convection there are still not understood well. In contrast, the Southwest Caribbean exhibits much more uniform ocean temperatures. The two regions together provide a broad range of atmospheric and sea surface conditions and a great deal of diversity in convective behavior. This served as the motivation for OTREC2019.

Flight operations for OTREC took place from August 5 to October 3, 2019. 22 research flights (127 research flight hours) over the East Pacific and Southwest Caribbean were performed out of Liberia, Costa Rica using the NSF/NCAR Gulfstream V aircraft. 655 dropsondes were deployed in a grid and the Hiaper Cloud Radar calculated data on cloudiness and precipitation below the aircraft. Radiosondes were launched from Santa Cruz and Limón (Costa Rica) and Nuqúi (Colombia) during the time period of OTREC. Intensified radiosonde launches were also executed at the standard radiosonde sites across Colombia. Additional weather and global positioning system column water vapor stations were established in Costa Rica and Colombia. Rainfall samples were collected in Costa Rica and Colombia.

Based on OTREC data, in this paper we present a preliminary look into thermodynamic parameters that might be good predictors of precipitation. We look at the correlation between the saturation fraction, that has well established relationship with precipitation, and the instability index as well as convective available potential energy (CAPE). We also show the vertical mass flux profiles for major convective events.

2 Data and Methods

The research flights took place in B1 and B2 boxes (shown in Figure 1) mostly on consecutive days to capture the passage of easterly waves. Box B1a was chosen to study Chóco jet, which impinges on the Pacific coast of Colombia and produces massive rainfall there (Poveda and Mesa, 2000), and possible initiation of easterly waves in that area (Kerns et al., 2008, Rydbeck and Maloney, 2015). Box B1b was chosen due to the uniform SST in the Caribbean and to study passage of easterly waves across Central America. Box B2 facilitated the study of Eastern Pacific ITCZ and convection in the area of strong meridional SST gradient as well as the passage of easterly waves from Southwest Caribbean and from the coast of Central America and Colombia.

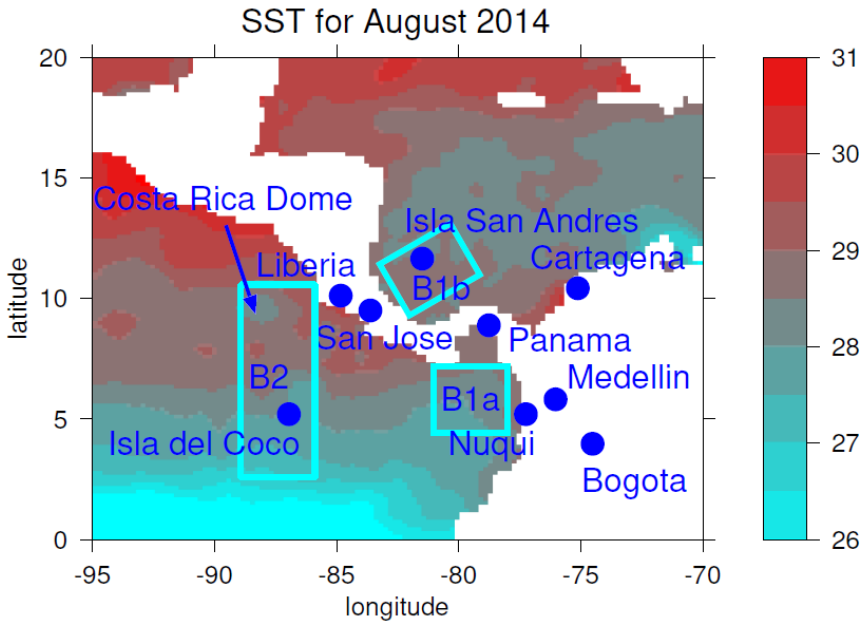

Figure 1. Flight area during OTREC.

Nine flights were performed in the Eastern Pacific off the coast of Colombia (box B1a) and in Southwest Caribbean (box B1b), while 12 flights were performed in the flight pattern B2 in the Eastern Pacific area. An additional flight was performed in collaboration with the National Oceanic Administration Hurricane Research Division P-3 while studying early stages of developing tropical storm Ivo. The main goal was to sample convection at all stages including the initial stage. The flight days were picked randomly in order to avoid selection bias. The B2 pattern was mainly flown a day after the B1 pattern to capture the passage of easterly waves.

Figure 2 shows examples of research flights (RF) executed in B1 (left) and B2 (right). The B1 pattern shows RF04 performed on August 16, 2019 (blue line) superimposed over a GOES-16

satellite longwave-IR image. Circles show the targeted dropsonde location used by our three-dimensional variational analysis (3DVAR) from which regular grids of data are derived (Lopez and Raymond, 2011, Elsberry and Harr, 2008, Raymond and Lopez, 2011, Raymond et al., 2011, Montgomery et al., 2012, Gjorgjievska and Raymond, 2014, Juracic and Raymond, 2016). Grid cell dimensions are 0.25 degree horizontally and 200 m vertically up to 16 km. The corresponding B2 pattern shows RF01 performed on August 07, 2019. The dataset for dropsondes used in this paper is NCAR/EOL AVAPS Dropsonde Quality Controlled Data Version 1.0.

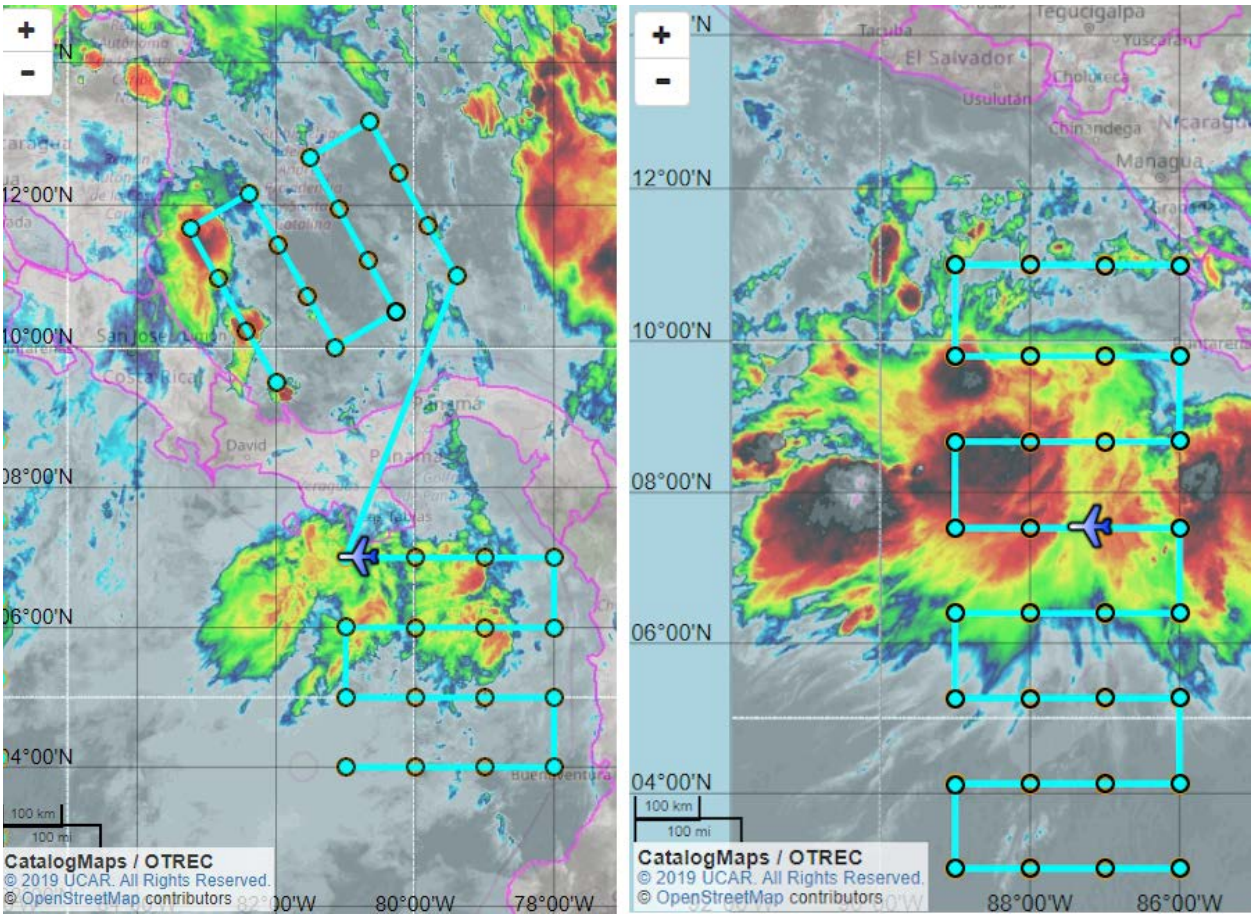

Figure 2. Flight pattern B1 flown on August 16, 2019 RF04 on the left, flight pattern B2 flown on August 7, 2019, RF01 shown on the right in blue lines superimposed over the GOES-16 satellite longwave-IR image. The locations of dropsondes are given by circles.

3 Results

Out of 9 flights performed in the B1 pattern, 5 convective cases were observed in B1a box and 3 in B1b box. Out of 12 flights performed in the B2 pattern, 8 convective cases were observed. The convective cases were defined subjectively by looking at GOES-16 satellite loops and images with the help of the log that we kept during the flight missions. Table 1 shows the summary of location, time and nature of the convective events that occurred during the OTREC flights. The goal is to look at the correlation between the thermodynamic indicators (convective available potential

energy and instability index) and the saturation fraction (good proxy for precipitation) for those convective events. We also look at the vertical mass flux profiles to see if they are related to thermodynamic variables.

3.1 Thermodynamic parameters

Figure 3 shows the scatter plot between CAPE and saturation fraction (left) and the instability index and saturation fraction (right) for all convective cases in B1a, B1b and B2 boxes. Each dot represents measurements from one dropsonde deployed within or around the convective event. Dropsonde data for B1a (the Colombian box) are given by red dots, for B1b (the Caribbean box) by blue dots and for B2 (the East Pacific box) by black dots. To calculate CAPE we used the SHARPpy python package (Blumberg et al., 2017) with 80 hPA mean surface layer parcel method.

Figure 3 tells an interesting story. CAPE and saturation fraction are only weakly anti-correlated with a correlation coefficient of 0.248. The anti-correlation between the saturation fraction and the instability index is more significant with a correlation coefficient of 0.607. Both correlations are valid at the 99% level. The slope of the anti-correlation between the saturation fraction and instability index, as seen subjectively from Figure 3, is different between the Colombian box and the other boxes. This is a subject of further research.

As saturation fraction is a good proxy for precipitation, it can be summarized that instability index is anti-correlated with precipitation and as such is a good environmental indicator for convection.

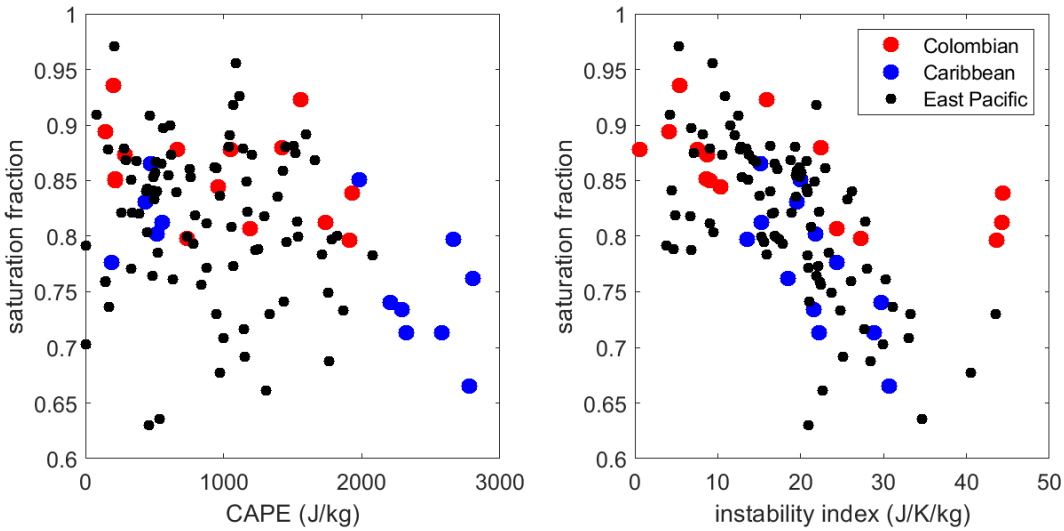

Figure 3. Scatter plot between the saturation fraction and CAPE on the left and saturation fraction and instability index on the right. Data for B1a Colombian box are given in red, for B1b Caribbean box in blue and for B2 East Pacific box in black.

3.2 Vertical mass flux profiles

Our 3DVAR analysis is used to create three-dimensional grids of data for each region of interest in Figure 1. After this the average mass flux profile is calculated only for the area with the convective event defined in Table 1. The vertical mass flux profile is defined as

$$M(z) = \overline{\rho w}$$

where ρ is the density and *w* is the vertical speed. Each convective event's vertical mass flux profile is given in a different color with a legend referring to the research flight during which the event had occurred. Every RF shown in Figure 4 had one convective event except RF14 that had two, see summary in Table 1. Bottom-heavy vertical mass flux profiles are given in solid lines, while top-heavy are given in dashed lines.

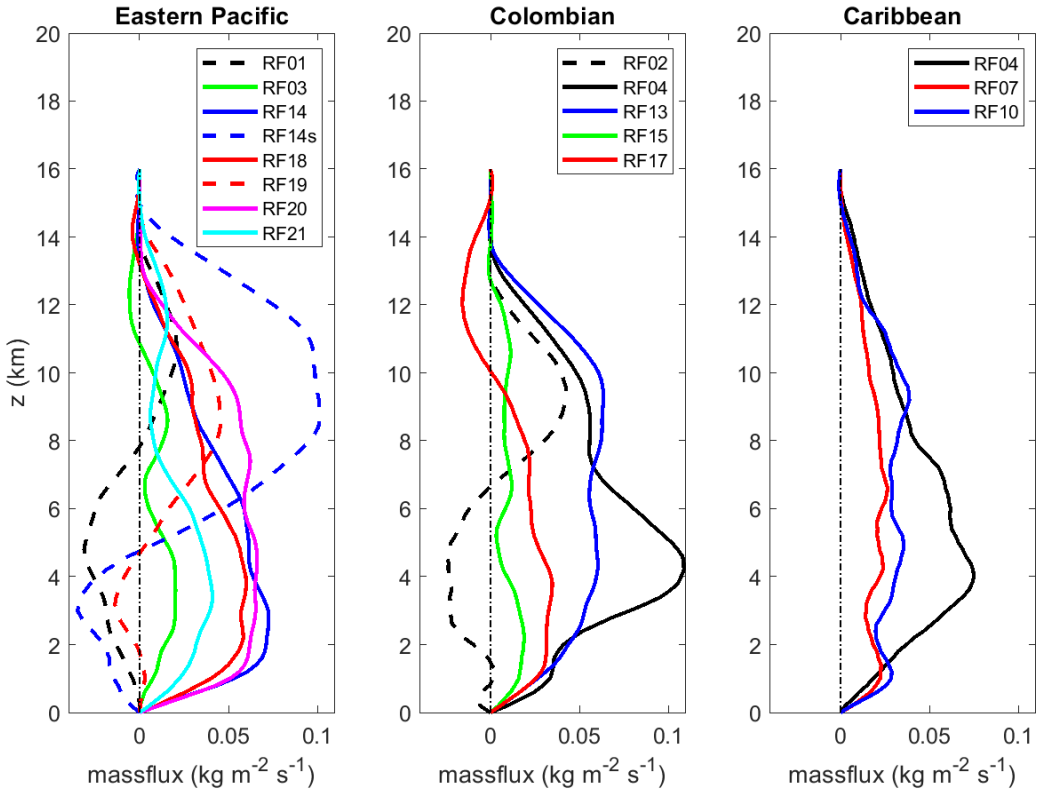

Figure 4. Vertical mass flux profiles for all convective cases Eastern Pacific B2 box, Colombian B1a box and Caribbean B1b box.

As with defining the convective systems, we subjectively separated growing from decaying convective systems using GOES-16 satellite loops, and mission reports and logs. Out of 8 convective cases in the Eastern Pacific box B2, we identify 5 cases that had developing convection and 3 cases that had decaying convection. Out of 5 convective cases in the Colombian box B1a, 3 cases had developing convection, 1 (RF04) had very pronounced shallow convection and 1 case (RF02) had mixed convection (decaying off the coast, otherwise developing). Out of 3 convective cases in the Caribbean box B1b all had developing convection. Regardless of location, every

developing case had a bottom-heavy vertical mass flux profile, while every decaying case had top-heavy mass flux profile. RF02 that exhibited signs of mixed convection was dominated by a top-heavy vertical mass flux profile.

4. Conclusions

Dropsonde data from the field project OTREC2019 is analyzed for 16 convective events that occurred in the Eastern Pacific and Southwest Caribbean during August 5 to October 3 of 2019. We looked at the thermodynamic parameters saturation fraction, instability index and CAPE as possible predictors of the local properties of environment upon which the development of convection is thought to be dependent. Saturation fraction is a kind of column relative humidity, while the instability index is a measure of the low to mid-level tropospheric moisture convective instability. This correlation between the saturation fraction and instability index is called moisture quasi-equilibrium, (Raymond et al., 2014). We find that CAPE and saturation fraction are weakly anti-correlated, while the instability index is more strongly anti-correlated with the saturation fraction for all convective cases, developing and decaying. We conclude that for all convective events and in all flight areas, the moisture quasi-equilibrium theory holds, though the slope of the regression curve is less for the Colombian region as can be seen subjectively from Figure 3.

3DVAR analysis is performed on the dropsondes grids and the vertical mass flux profiles are calculated. Out of 16 convective cases, 11 had developing convection and 3 decaying convection. One case showed signs of mixed convection, developing and decaying. One case was shallow convection only. All developing cases, in Eastern Pacific, Southwest Caribbean and off the coast of Colombia had bottom-heavy vertical mass flux profile, while all decaying ones had the top-heavy profile.

Further research is planned to understand the reasons for the decrease in instability index, its relationship to bottom-heavy vertical mass flux profiles and the possible differences between the Eastern Pacific, Southwest Caribbean and Colombian box.

Table 1. Summary of location, time and nature of the convective events that occurred during the OTREC flights.

Research Flight	Date	Location	Description	Vertical Mass Flux Profile
B1a Colombian box: Convective events				
02	08/11/2019	-81 to -78 W 5.5 to 7 N	Developing Decaying: off the coast	top
04	08/16/2019	-81 to -78 W 5.5 to 8 N	Shallow convection	bottom
13	09/17/2019	-81 to -78 W 4 to 7 N	Developing	bottom
15	09/22/2019	-81 to -78 W 5.5 to 7 N	Developing	bottom
17	09/25/2019	-81 to -78 W 3.5 to 8 N	Developing	bottom
B1b Caribbean box: Convective events				
04	08/16/2019	-83 to -81 W 9 to 11 N	Developing	bottom
07	08/22/2019	-83 to -79.5 W 9.5 to 11.5 N	Developing	bottom
10	09/03/2019	-83 to -79.5 W 9 to 11 N	Developing	bottom
B2 Eastern Pacific box: Convective events				
01	08/07/2019	-89 to -86 W 6 to 11 N	Decaying at the flight time, later became tropical storm Henriette	top
03	08/12/2019	-89 to -86 W 8 to 11 N	Developing	bottom
14	09/21/2019	-89 to -86 W 7 to 9.5 N	Developing	bottom
14s	09/21/2019	-89 to -86 W 10 to 12 N	Decaying	top
18	09/27/2019	-89 to -86 W 10 to 11 N	Developing	bottom
19	09/28/2019	-89 to -86 W 6 to 10 N	Decaying	top
20	09/30/2019	-89 to -86 W 3 to 6 N	Developing	bottom
21	10/01/2019	-89 to -86 W 7 to 10 N	Developing	bottom

Acknowledgments, Samples, and Data

We would like to acknowledge operational, technical and scientific support provided by NCAR's Earth Observing Laboratory, sponsored by the National Science Foundation. The NCAR/EOL AVAPS Dropsonde QC Data DOI: https://doi.org/10.26023/EHRT-TN96-9W04. Data is provided by NCAR/EOL under the sponsorship of the National Science Foundation https://data.eol.ucar.edu/. This work was supported by National Science Foundation grant 1758513.

References

Back, L. E., & Bretherton, C. S. (2009), On the relationship between SST gradients, boundary layer winds, and convergence over the tropical oceans, *Journal of Climate, 33*, 4182-4196.

Battisti, D. S., Sarachik, E. S., & Hirst, A. C. (1999), A consistent model for the large-scale steady surface atmospheric circulation in the tropics, *Journal of Climate, 12*, 2956-2964.

Blumberg, W.G., Halbert, K.T., Supinie, T.A., Marsh, P.T., Thompson, R.L., & Hart, J.A. (2017), SHARPpy: An Open-Source Sounding Analysis Toolkit for the Atmospheric Sciences, *Bulletin of the American Meteorological Society, 98*, 1625–1636, https://doi.org/10.1175/BAMS-D-15-00309.1

Bretherton, C.S., Peters, M.E., & Back, L.E. (2004), Relationships between Water Vapor Path and Precipitation over the Tropical Oceans. *Journal of Climate*, **17**, 1517–1528, https://doi.org/10.1175/1520-0442(2004)017<1517:RBWVPA>2.0.CO;2

Elsberry, R. L. & Harr, P. A. (2008), Tropical cyclone structure (TCS08) field experiment science basis, observational platforms, and strategy, *Asia-Pacific Journal of Atmospheric Sciences*, *44*, 209–231.

Emanuel, K. A. (1986), An air-sea interaction theory for tropical cyclones. Part I: Steady state maintenance, *Journal of Atmosperic Sciences*, *43*, 585-604.

Emanuel, K. A., (1987), An air-sea interaction model of intraseasonal oscillations in the tropics, *Journal of Atmosperic Sciences*, *44*, 2324-2340.

Gjorgjievska, S. & Raymond, D. J. (2014), Interaction between dynamics and thermodynamics during tropical cyclogenesis, *Atmospheric Chemistry and Physics*, 14, 3065-3082.

Juračić, A., & Raymond, D. J. (2016): The effects of moist entropy and moisture budgets on tropical cyclone development, *Journal of Geophysical Research*, 121, 9458-9473.

Kerns, B., Greene, K., & Zipser, E. (2008), Four Years of Tropical ERA-40 Vorticity Maxima Tracks. Part I: Climatology and Vertical Vorticity Structure, *Monthly Weather Review, 136*, 4301–4319, https://doi.org/10.1175/2008MWR2390.1

Lindzen, R. S., & Nigam, S. (1987), On the role of sea surface temperature gradients in forcing low-level winds and convergence in the tropics, *Journal of Atmospheric Sciences*, *44*, 2418-2436.

Lopez Carrillo, C., & Raymond, D. J. (2011), Retrieval of three-dimensional wind fields from Doppler radar data using an efficient two-step approach, *Atmospheric Measurement Techniques*, *4*, 2717-2733, doi:10.5194/amt-4-2717-2011.

Montgomery, M. T., Davis, C., Dunkerton, T., Wang, Z., Velden, C., Torn, R., Majumdar, S. J., Zhang, F., Smith, R. K., Bosart, L., Bell, M. M., Haase, J. S., Heymsfield, A., Jensen, J., Campos, T., & Boothe, M. A. (2012), The Pre-Depression Investigation of Cloudsystems in the Tropics (PREDICT) experiment, *Bulletin of the American Meteorological Society*, *93*, 153–172.

Neelin, J. D., Held, I. M., & Cook, K. H. (1987), Evaporation wind feedback and low-frequency variability in the tropical atmosphere, *Journal of Atmospheric Sciences*, *44*, 2341-2348.

Poveda, G., & Mesa, O. J. (2000), On the existence of Lloró (the rainiest locality on Earth): Enhanced ocean-land-atmosphere interaction by a low-level jet, *Geophysical Research Letters*, *27*, 1675-1678, https://doi.org/10.1029/1999GL006091

Raymond, D. J., Esbensen, S. K., Paulson, C., Gregg, M., Bretherton, C. S., Petersen, W. A., Cifelli, R., Shay, L. K., Ohlmann, C., & Zuidema, P. (2004), EPIC2001 and the coupled ocean-atmosphere system of the tropical east Pacific, *Bulletin of the American Meteorological Society*, 85, 1341-1354.

Raymond, D. J., S. L. Sessions, and C. Lopez Carrillo, 2011: Thermodynamics of tropical cyclogenesis in the northwest Pacific, *Journal of Geophysical Research*, 116, D18101, doi:10.1029/2011JD015624.

Raymond, D. J., & Lopez Carrillo, C. (2011), The vorticity budget of developing typhoon Nuri (2008), *Atmospheric Chemistry and Physics*, *11*, 147-163, doi:10.5194/acp-11-147-2011.

Raymond, D. J., Gjorgjievska, S., Sessions, S., & Fuchs, Ž. (2014), Tropical cyclogenesis and mid-level vorticity, *Australian Meteorological and Oceanographic Journal*, *64*, 11-25.

Raymond, D. J. (2017), Convection in the east Pacific intertropical convergence zone, *Geophysical Research Letters*, *44*, 562-568, doi:10.1002/2016GL071554.

Riehl, H., Yeh, T. C., Malkus, J. S., & La Seur, N. E. (1951), The north-east trade of the Pacific ocean, *Quarterly Journal of the Royal Meteorological Society*, *77*, 598-626.

Rydbeck, A.V., & Maloney, E.D. (2015), On the Convective Coupling and Moisture Organization of East Pacific Easterly Waves, *Journal of Atmospheric Sciences*, *72*, 3850–3870, https://doi.org/10.1175/JAS-D-15-0056.1

Stevens, B., Duan, J., McWilliams, J. C., Munnich, M., & Neelin, J. D. (2002), Entrainment, Rayleigh friction, and boundary layer winds over the tropical Pacific, *Journal of Climate*, *15*, 30-44.

Tomas, R. A., Holton, J. R., & Webster, P. J. (1999), The influence of cross-equatorial pressure gradients on the location of near-equatorial convection, *Quarterly Journal of the Royal Meteorological Society*, *125*, 1107-1127.

UCAR/NCAR - Earth Observing Laboratory, Voemel, H. (2019), NCAR/EOL AVAPS Dropsonde QC Data. Version 1.0. UCAR/NCAR - Earth Observing Laboratory. https://doi.org/10.26023/EHRT-TN96-9W04. Accessed 13 January 2020.

Yano, J.-I., & Emanuel, K. (1991), An improved model of the equatorial troposphere and its coupling with the stratosphere, *Journal of Atmospheric Sciences*, *48*, 377-389.